参赛队员姓名：何承堃、陈天弈

中学：南京外国语学校

省份：江苏省

国家/地区：中华人民共和国

指导教师姓名：郭子建、许亮亮

论文题目：**Novel 4D-Coding System Based on Circularly Polarized Luminescent Pt Complexes**

（基于圆偏振发光铂配合物的四维码构建）

本参赛团队声明所提交的论文是在指导老师指导下进行的研究工作和取得的研究成果。尽本团队所知，除了文中特别加以标注和致谢中所罗列的内容以外，论文中不包含其他人已经发表或撰写过的研究成果。若有不实之处，本人愿意承担一切相关责任。

参赛队员：　　　　　　指导老师：

2020　年　09 月　09 日

基于圆偏振发光铂配合物的四维码构建

何承堃，陈天弈

中文摘要

在三维码基础上通过增加色彩编码新维度构建四维码(4D code)可为人工智能时代的数据加密和信息储存密度提升提供重要支持，因此相关研究广受关注。自然界甲虫的反射圆偏振光(RCPL)呈圆偏振器依赖的颜色变化。基于手性染料所发射圆偏振光(CPL)的相似特点及其波长依赖的偏振椭圆度，我们提出了手性染料圆偏振发光经过四分之一波片/线偏振器组合实现圆偏振发光色彩变化的四维码构建思路。为获得合适的圆偏振发光染料，我们通过研究手性对映体铂配合物(*R*)-和(*S*)-**BTPt** 的圆偏振发光性能，发现(*R*)-或(*S*)-**BTPt** 在聚甲基丙烯酸甲酯(PMMA)薄膜基质可自组装形成四聚体，使其圆偏振发光 g_{lum} 因子达到 0.88(R-构型)和 0.67(S-构型)。优异的圆偏振发光性能使得该铂配合物掺杂的 PMMA 薄膜受激后发光经四分之一波片/线偏振器组合后呈现了明显的色彩变化，并依赖于四分之一波片和线偏振器间旋转角的变化。进一步我们利用(*R*)-**BTPt** 和其他染料分别掺杂 PMMA 薄膜并通过组合构建了基于圆偏振发光的四维码。由于(*R*)-**BTPt** 色块的 CPL 变色性能，该码在不同旋转角下出现不同的颜色组合。这一依赖于旋转角的颜色组合信息，为信息加密和编码提供了第四维编码手段。利用圆偏振发光染料(*S*)-**BTPt** 和普通染料掺杂的PMMA溶液分别书写字母也显示了旋转角依赖的不同色彩的字母组合。这些依赖于四分之一波片和线偏振器间旋转角的色彩变化表明利用高 g_{lum} 因子圆偏振发光染料替代普通染料调制三维码色块是构建四维码的可靠新途径，在信息加密提升和防伪等方面具有良好的应用前景。而发展不同发射颜色的圆偏振发光染料及其对映体将为这种基于圆偏振发光的四维码技术提供更大的发展空间。

关键词： 四维码 (4D Code), 色彩(Colour), 圆偏振发光(Circularly polarized luminescence), 铂配合物(Pt complex), 聚甲基丙烯酸甲酯(PMMA), 手性染料(Chiral dyes)

Novel 4D-Coding System Based on Circularly Polarized Luminescent Pt Complexes

Chengkun He (何承堃), Tianyi Chen (陈天弈)

Abstract

Developing a 4D-coding system via adding new dimensional coding technique for colour in 3D codes is attracting much more interests, since it offers high security and capacity in data storage and communication for the era of artificial intelligence. Inspired by circular polarizer-dependent colours of reflected circularly polarized light (RCPL) from beetles, we proposed a coding technique for the colour of chiral dyes' circularly polarized luminescence (CPL) for 4D coding, considering CPL's wavelength-dependent polarization ellipticity and similarity to RCPL. In this proposal, a filter setup composed by a quarter-wave plate and a linear polarizer will be adopted to visualize CPL colour change. To acquire suitable CPL dyes for this purpose, we investigated the CPL behaviours of two enantiomeric Pt complexes, (*R*)- and (*S*)-**BTPt**, and found that (*R*)- or (*S*)-**BTPt** self-aggregated to form tetramers in PMMA matrix to emit CPL with large g_{lum} values (0.88 for *R*-form). Irradiating PMMA films doped with (*R*)- or (*S*)-**BTPt** displayed obvious CPL colour change with the filter setup changing the rotational angle between the quarter-wave plate and linear polarizer. Then CPL-based 4D code was prepared via doping PMMA matrixes respectively with (*R*)-**BTPt** and other dyes. The CPL colour change of (*R*)-**BTPt**-doped matrix caused by rotational angle variation led to the different colour combinations. These colour combinations provided the 4th dimensional information for 4D coding and data encryption. Writing letters with (*S*)-**BTPt**- or normal dye-containing PMMA solutions showed also the different letter colour combinations at different rotational angles. All the rotational angle-dependent colour changes of CPL indicated that replacing normal dyes with CPL dyes of large g_{lum} values to modulate colour matrix of 3D codes is new promising approach to 4D coding and anti-counterfeiting data encryption. Developing CPL dyes of different colours and their enantiomers would lead to more space for this CPL-based 4D-coding technique.

Keywords: 4D Code, Colour, Circularly polarized luminescence, Pt complex, PMMA, Chiral dyes

Contents (目录)

Introduction

Different from the 1D- and 2D-coding techniques which depend respectively on lines/spaces and matrix/stacking, 3D coding depends on colour coding of matrix modules. Although 3D coding enhances distinctly the data storage density and security, the coming era of artificial intelligence demands significant promotion in information storage and communication.[1] Therefore, developing additional dimension of coding techniques for data encryption and storage capacity promotion are now attracting much more interest,[2] and the new dimensional coding techniques for colour is a promising alternative. An and co-workers have reported a new dimensional colour coding strategy showing the lifetime-dependent luminescence colour.[3] This indicates that discriminating luminescence colours according to their intrinsic nature such as lifetime may offer a new dimensional colour coding technique, and exploring light intrinsic properties differentiable by a suitable detector would be helpful to construct novel 4D-coding techniques based on the 3D-coding system.

Circularly polarized luminescence (CPL) from chiral luminophores or assemblies is a nature gift for people to manipulate circularly polarized light for 3D displays,[4] information storage and processing,[5] and spin information communicating.[6] To construct a novel 4D-coding system, we proposed a new dimensional coding method for CPL colour. This method utilizes a filter setup, composed by a quarter-wave plate and a linear polarizer, to show CPL colour change through changing the rotational angle (θ) between two components of this setup (Scheme 1). We then investigated the CPL activity of two enantiomeric Pt(II) complexes, (*R*)-/(*S*)-**BTPt**, with the purpose to acquire suitable CPL dyes for 4D coding. Both complexes emitted strong CPL in PMMA (poly(methylmethacrylate)) films with large luminescence dissymmetry factors (g_{lum}) via forming tetramer assemblies. This CPL showed colour change after passing through the filter setup at different θ. We then prepared the CPL-based 4D code via doping PMMA matrixes respectively with (*R*)-**BTPt** and other dyes. The CPL colour change of (*R*)-**BTPt**-doped matrix led to the different colour combinations at different rotational angles. These colour combinations provided the

4th dimensional information for 4D coding and data encryption. This result confirms a promising approach to 4D coding and data encryption via replacing normal dyes with CPL dyes of large g_{lum} values to modulate colour matrix of 3D codes.

Results and discussion

Idea of 4D coding with circularly polarized luminescent dyes

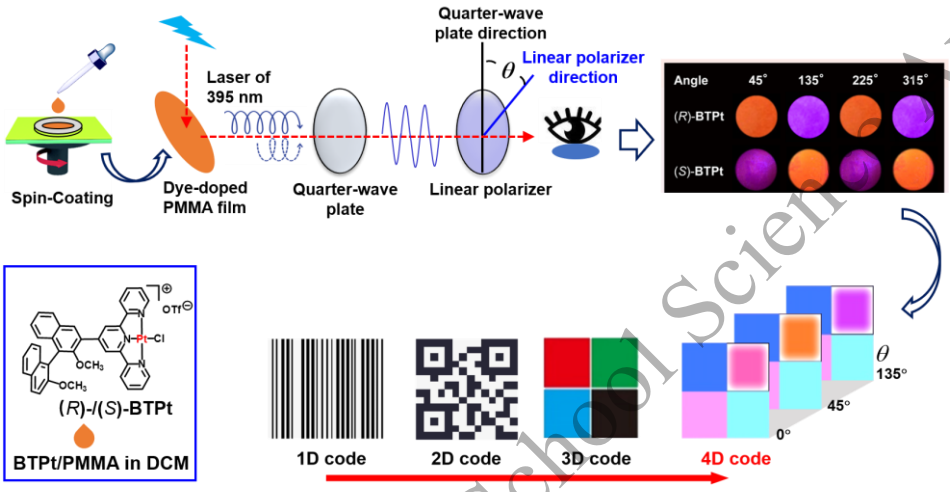

Scheme 1. Schematic illustration of a 4D-coding system based on the circularly polarized luminescence of (*R*)-/(*S*)-**BTPt** in PMMA spin-coating films. CPL colour change of the two complexes can be visualized by a filter setup composed by a quarter-wave plate and a linear polarizer via changing the rotational angle (θ). Doping PMMA film with **BTPt** and other dyes leads to the additional θ-dependent colour information over normal 3D codes.

From the literature, we noted that the left and right circular polarizers made beetles' reflected left-handed circularly polarized light show different colors.[7] The chiral ordering of beetle's exoskeleton cells due to the local curvature has been proposed as the origin for this left-handed reflected circularly polarized light (RCPL), while the circular polarizers act as detectors to visualize light polarity as different colors. Considering the similarity of CPL to RCPL, we proposed a new dimensional coding technique for CPL color using a filter setup, composed by a quarter-wave plate and a linear polarizer. With the wavelength-dependent polarization ellipticity of CPL, the light composition after CPL passing through this setup would be changed at different rotational angle, θ, to show color variation.

Therefore, we proposed herein a new 4D coding system using CPL dyes other than

normal dyes to write 3D codes, and the circular polarity of CPL from chiral dyes would be displayed by the filter setup to show varied colors at different θ (Scheme 1). The g_{lum} value of most reported CPL dyes is in the range of 10^{-3}-10^{-2},[8] which are not large enough to make CPL polarity distinguishable by this filter setup. Therefore, CPL dyes of large g_{lum} values are preferred for this new 4D coding systems. Prof. Guo and co-workers have just developed a pair of luminescent Pt(II) complex enantiomers formed by (*R*)- and (*S*)-1,1'-binapthalylterpyridine (**BINPTP**, **BT**), (*R*)- and (*S*)-**BTPt**. The two complexes tend to form dimers and tetramers in the crystal state and show intensive ^{3}MMLCT (metal-metal-to-ligand charge transfer) luminescence. Since the complexes' assembly chirality and ^{3}MMLCT luminescence inferred fine CPL activity, we then investigated the CPL behaviour of these two Pt complexes in different media, and constructed successfully the CPL-based 4D codes using (*R*)-**BTPt** and other dyes in PMMA films in the final.

CPL behaviours of complexes (R)-/(S)-BTPt in solutions and PMMA films

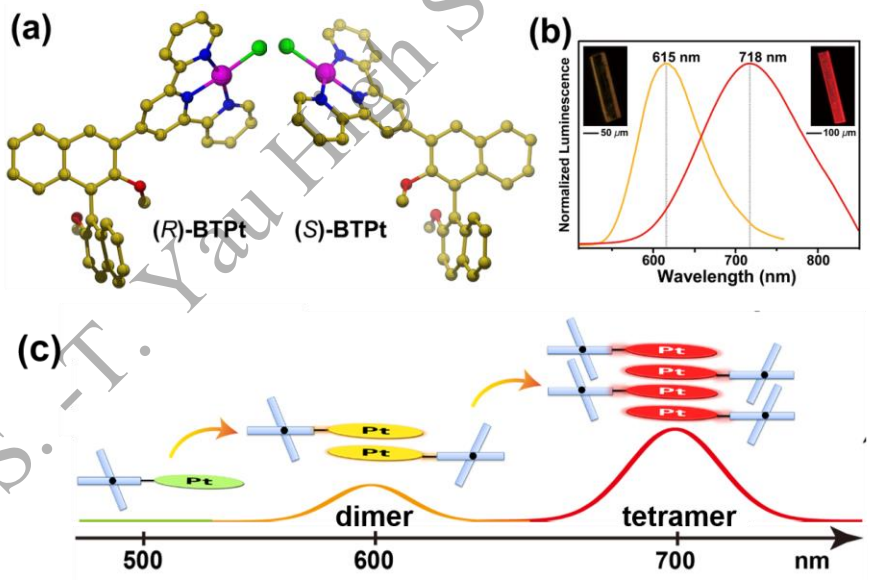

Figure 1. (a) Molecular structure of (*R*)- and (*S*)-**BTPt**. Anion and protons were omitted for clarity; (b) luminescence spectra of orange- and red-emissive single crystals of **BTPt**. λ_{ex}, 380 nm. Inset: photograph of orange- and red-emissive crystals under UV lamp of 365 nm; (c) schematic illustration of luminescence originating from dimers and tetramers of **BTPt**.

Luminescence behaviours in the solid state. Two kinds of single crystals, the orange- and red-emissive crystals, have been obtained for (*R*)- and (*S*)-**BTPt**

complexes. In orange-emissive crystals, complex cations, $[Pt(BT)Cl]^+$, tend to form dimers which self-assembly to form one dimensional chain. These orange-emissive crystals luminesce weakly with a broad band (540-780 nm) showing a maximum at ~ 615 nm (Figure 1b). This band can be assigned as the ^{3}MMLCT emission of dimers. In red-emissive crystals, the complex cations tend to form tetramers, which self-assembly also to form one dimensional chain. These crystals emit red luminescence strongly showing a broad emission band (550-900 nm) with a maximum at ~718 nm (Figure 1b), which can be assigned as the ^{3}MMLCT emission of tetramers. Structure analysis found the complicated helix assembly of binaphthalene moiety. Such a supramolecular chirality normally leads to high g_{lum} values according to many CPL reports.[9] With the ^{3}MMLCT luminescence found for dimers and tetramers, especially the strong tetramer luminescence, we expected the fine CPL activity of both (*R*)- and (*S*)-**BTPt** tetramer assemblies. However, acquiring bulk crystals large enough for CPL determination and application is challenging.

Aggregation and CPL behaviours in solutions. Considering (*R*)- and (*S*)-**BTPt** molecules might aggregate in solvents similar to AIE phenomenon in solution,[10] we determined CPL of both complexes in solution. Both (*R*)- and (*S*)-**BTPt** show no obvious emission in solvents such as CH_2Cl_2 (DCM), DMSO, DMF, and CH_3OH, except for the negligible ligand emission at ~430 nm (Figure 2a). The absence of ^{3}MMLCT luminescence indicated there was no $[Pt(BT)Cl]^+$ aggregate such as dimer and tetramer. In nonpolar solvents of low complex solubility such as hexane and cyclohexane, we found the distinct luminescence band centered at ~710 nm, which is comparable to that of tetramers in red-emissive crystals. This phenomenon inferred the tetramer formation in hexane. This aggregation behaviour was confirmed by adding hexane into DCM solutions of both (*R*)- and (*S*)-**BTPt**, which revealed both complexes began to show excimer emission when the volumetric fraction of hexane (f_h) became above 50% (Figure 2b). Increasing f_h to 70% made the luminescence gradually shift to ~710 nm and increase to its maximum. The final emission band is similar to the luminescence of tetramers found in the solid state. All these indicated that **BTPt** complex tended to form aggregates such as tetramers when decreasing their

solubility in DCM by adding hexane, and CPL ascribed to these aggregates was observed.

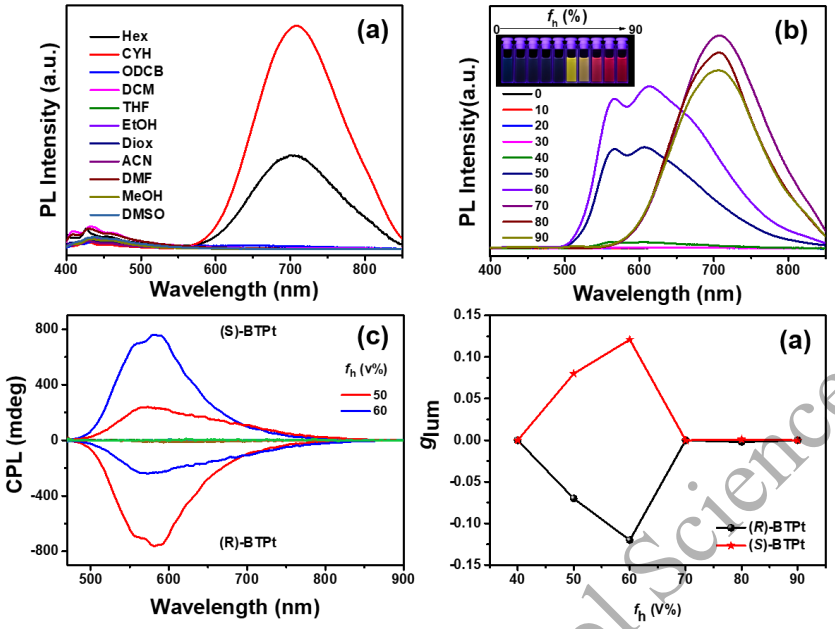

Figure 2. (a) Luminescence spectra of (*R*)**-BTPt** (1×10^{-5} mol L^{-1}) in different solvents; (b) luminescence spectra of **(***R***)-BTPt** (1×10^{-5} mol L^{-1}) in DCM/hexane binary solvent systems with varied volumetric fractions of hexane (f_h); inset in (b): photograph of solutions with varied f_h showing luminescence color change under UV lamp of 365 nm. (c) CPL spectra and (d) g_{lum} values of (*R*)- and (*S*)**-BTPt** (1×10^{-4} mol L^{-1}) in DCM/hexane binary solvent systems determined with varied f_h. λ_{ex}, 380 nm.

CPL spectra determination of (*R*)- and (*S*)**-BTPt** in DCM showed no CPL signal at all, yet the determination in DCM/hexane binary solvent systems revealed that the CPL signal (maximum at ~ 590 nm) appeared only when f_h attained to 50%, and this broad CPL band (500-800 nm) reached its maximum when f_h attained to 60%, resulting in a $|g_{lum}|$ value increment from 0 to 0.12 (Figures 2c and 2d). This broad CPL band decreased distinctly when f_h became higher than 70%, and the precipitation of large aggregates might be the origin. There was no CPL band at ~710 nm for both (*R*)- and (*S*)**-BTPt** in all f_h range, which is inconsistent with the luminescence spectra showing distinct emission band at 710 nm at high f_h (Figure 2a). This inconsistency can be ascribed to the aggregate precipitation at high f_h and the different data collection times (luminescence spectrum, ~ 30 s; CPL spectrum, >20 mins). As the tetramer luminescence at ~710 nm was stronger than the dimer luminescence at 590 nm in the solid state, searching for a new system to stabilize tetramer aggregates

might lead to stronger CPL signal at ~710 nm, favouring 4D-coding application.

CPL behaviour in PMMA matrix. Many studies have displayed that PMMA and other polymer films might be a suitable matrix to stabilize luminophore aggregates. Therefore, we investigated the luminescent behaviour of (*R*)- and (*S*)-**BTPt** in PMMA film. The films were prepared via spin-coating PMMA solutions containing variable Pt complex fractions on quartz plates. The films containing 0.1-1% (mass fraction, wt%) (*R*)- or (*S*)-**BTPt** showed only weak luminescence with a band of a maximum at ~560 nm, inferring the formation of dimer aggregates in the film (Figure 3a). Increasing mass fraction of Pt complex to 5% made the film show dual luminescence bands at ~560 and 720 nm, suggesting tetramer aggregates had also formed. Further increasing mass fraction of Pt complex led to the general enhancement of luminescence band at 720 nm, and this band became the dominated one at Pt complex mass fraction of 30%, inferring the tetramer aggregates became the main aggregate form in PMMA films.

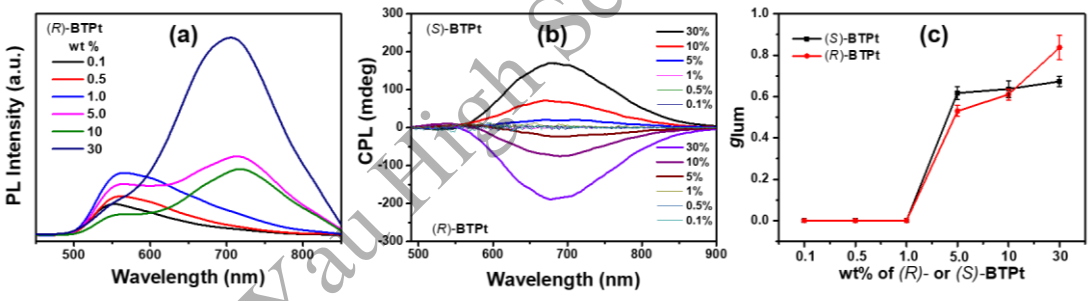

Figure 3. (a) PL and (b) CPL spectra of (*R*)-**BTPt** in PMMA films containing different mass fraction (wt%) of Pt complex; (c) $|g_{lum}|$ values of (*R*)- and (*S*)-**BTPt** in PMMA films determined at different wt%. λ_{ex}, 380 nm.

Then we determined the CPL spectra and g_{lum} values of (*R*)- and (*S*)-**BTPt** in PMMA films respectively. To avoid interference of linearly polarized light, the $|g_{lum}|$ values were determined via measuring circularly polarized luminescence spectra using a fluorescence spectrofluorometer modified with a rotatable quarter-wave plate and a rotatable linear polarizer, and cesium tetrakis(3-heptafluoro-butylryl-(+)-camphorato)Eu(III) complex (Cs[Eu((+)-hfbc)$_4$]) in $CHCl_3$ was utilized as the reference.[11] CPL spectra determination revealed the concentration-dependent CPL for both *R*- and (*S*)-**BTPt** in PMMA films (Figure 3b).

The films showed no CPL signal when mass fraction of (*R*)- and (*S*)-**BTPt** was in the range of 0.1 to 1.0. When the mass fraction of Pt complex increased to 5.0%, both (*R*)- and (*S*)-**BTPt** showed a CPL band at ~700 nm, which appeared as a pair. Determination revealed also the large $|g_{lum}|$ values of ~0.51 for (*R*)-**BTPt** and 0.61 for (*S*)-**BTPt**. The CPL intensity increased distinctly with the mass fraction of Pt complex increasing from 1.0% to 30%, and the $|g_{lum}|$ values at 30% fraction were determined as 0.88 for (*R*)-**BTPt** and 0.67 for (*S*)-**BTPt**. To the best of our knowledge, the $|g_{lum}|$ value of 0.88 is the largest one in the reported CPL materials except for the lanthanide(III) complexes. All these indicated that both (*R*)- and (*S*)-**BTPt** were inclined to form aggregates especially tetramers in PMMA films. This self-assembly behaviour in PMMA film and the associated CPL properties offer the promising potential of the two Pt complexes in applications such as 4D coding.

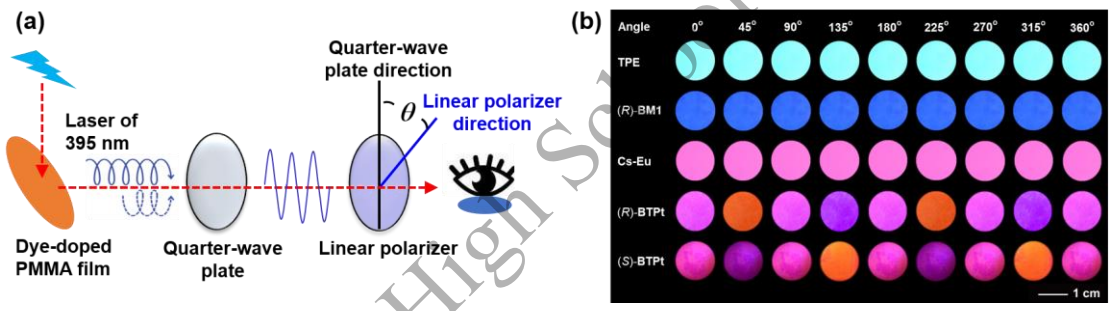

Figure 4. (a) Schematic illustration of experimental setup to distinguish CPL of (*R*)- and (*S*)-**BTPt** in PMMA films: a quarter-wave plate and a linear polarizer were arranged in line. The excitation light pathway is perpendicular to the luminescence pathway for detection. (b) Polarization-resolved luminescence colors of TPE, (*R*)-BM1, Cs[Eu((+)-hfbc)$_4$] (Cs-Eu), and (*R*)-/(*S*)-**BTPt** in PMMA films. The rotational angle (θ) was increased from 0 °to 360 °.

4D coding and data encryption with complexes (R)-/(S)-BTPt

Considering the large g_{lum} values of the two complexes in PMMA films, we supposed that the CPL of (*R*)-/(*S*)-**BTPt** aggregates in films could be distinguished using circularly polarized filters. We utilized a filter setup, which is a combination of a quarter-wave plate and linear polarizer, to verify our assumption (Figure 4a). Therefore, the CPL from the doped PMMA films would pass through the quarter-wave plate and result in linearly polarized light. The linearly polarized light then passing through the linear polarizer at a suitable rotational angle (θ) between the

quarter-wave plate and linear polarizer, and the polarity difference of CPL can be distinguished by showing variable luminescence colors and intensities at different θ.

The irradiated (*R*)-/(*S*)-**BTPt** (30%) in PMMA films gave luminescence intensity maximum at θ of 45° and 225° for (*R*)-**BTPt**, and 135°/315° for (*S*)-**BTPt**, showing the luminescence colors of orange and purple (Figure 4b). However, there was no linearly polarized light detectable at $\theta = n\times90°$ (n = 0, ±1, ±2……), showing only the background color of non-polarized luminescence as magenta. Therefore, the rotating linear polarizer led to the cycle of color change from magenta (0°) to orange (45°) to purple (135°) to magenta (180°) for (*R*)-**BTPt**, while the cycle of color change for (*S*)-**BTPt** is magenta (0°) to purple (45°) to orange (135°) to magenta (180°). A control experiment with tetraphenyl ethylene (TPE) doping disclosed that TPE assemblies in PMMA films showed bright cyan upon laser irradiation. Varying the rotational angle resulted in no obvious change in luminescence color and intensity, indicating the recorded cyan is the background color of nonpolarized luminescence of TPE. This is consistent with the achiral nature of TPE. In addition, CPL dye (*R*)-BM1 showed also no change in emission color (blue) and intensity upon varying rotational angle. This can be ascribed to its low CPL nature ($g_{lum} = 1.7\times10^{-3}$). This phenomenon indicated that only CPL dyes of high g_{lum} displayed the change of luminescence intensity and colour with this experimental setup. Although Cs[Eu((+)-hfbc)$_4$] has large g_{lum} value in both chloroform solution (1.38) and aggregation state (1.41), it retained its luminescence colour of pink at a different rotational angle and showed only the intensity change. The very sharp CPL band of Cs[Eu((+)-hfbc)$_4$] might be the origin. Both (*R*)- and (*S*)-**BTPt** displayed a broad CPL band from 550-900 nm, the g_{lum} values at different luminescence wavelengths of CPL band are different,[12] and CPL passing through the filter setup would result in different wavelength compositions at a different rotational angle, showing the θ-dependent color changes (Figure 5).

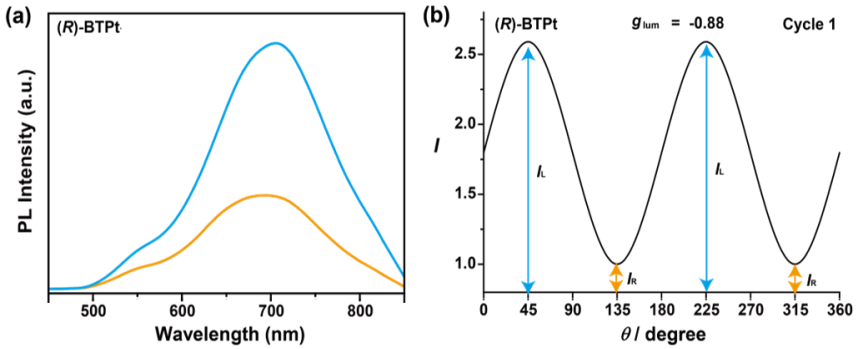

Figure 5. (a) Luminescence spectra and (b) plot of luminescence intensity at 720 nm of (*R*)-**BTPt** in PMMA film determined at different rotational angle (θ) between quarter-wave plate and linear polarizer. The Pt complex mass fraction in the film was 30%.

With the luminescence colour change of **BTPt** complexes demonstrated by circularly polarized filters, we utilized this CPL dye to replace normal dye to prepare 3D code for 4D coding and encryption. We doped PMMA films respectively with (*R*)-**BTPt** (top left), TPE, (*R*)-BM1, and Cs[Eu((+)-hfbc)$_4$] and then joined the films regularly to form a "3D" code (Figure 6a). The decryption was realized by demonstrating the luminescence color change of the "3D" code via changing rotational angle. When θ was at 0 °, 90 °, 180 °, 270 °, or 360 °, 3D code displayed always four different colors, magenta from (*R*)-**BTPt**, cyan from TPE, pink from Cs[Eu((+)-hfbc)$_4$], and blue from (*R*)-BM1, respectively. This can be programmed as Code I, and the readout information was defined as false information (false info). After changing θ to 45 ° or 225 °, the matrix with (*R*)-**BTPt** showed the color of orange, resulting in a new 3D code as Code II, and information A (info A) was readout. When θ subsequently being varied to 135° or 315°, this "3D" code displayed four colors of purple, cyan, pink and blue, which was programmed as Code III, and then information B (info B) was readout. Consequently, a new 4D code could be generated by integrating Code I, II, and III, resulting in information C (info C) with a high level of security.

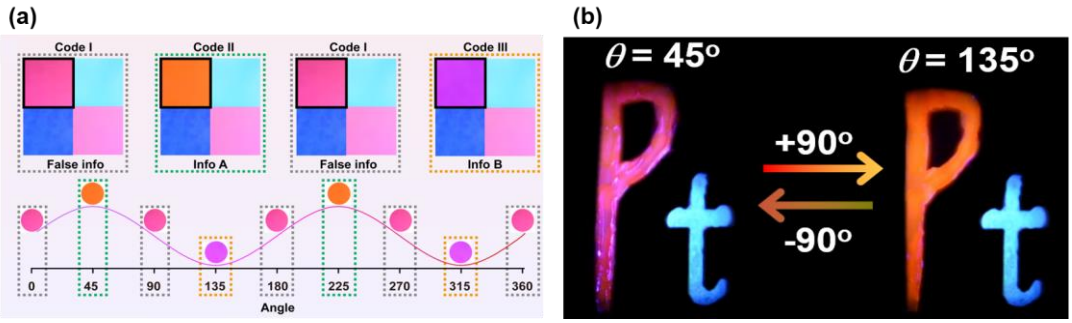

Figure 6. 4D data encryption/decryption with (*R*)- and (*S*)-**BTPt**. (a) 4D code constructed via doping PMMA film with CPL dye (*R*)-**BTPt** (top left), SPE (top right), (*R*)-BM1 (bottom left), and Cs[Eu((+)-hfbc)$_4$] (bottom right). The code images were recorded at different rotational angles. λ_{ex}, 395 nm. (b) Illustration of CPL-encoding for security improvement using (*S*)-**BTPt** (for "P") in combination with **TPE** (for "t") to write word "Pt". The encrypted feature of "P" can be identified by naked eyes via changing rotational angle (θ) from 45° (purple "P") to 135° (orange "P"). λ_{ex}, 365 nm.

The successful 4D-coding based on CPL of **BTPt** suggested that **BTPt** assemblies in PMMA might be used in document security. Therefore, the two letters of word "Pt", "P" and "t", written on a quartz plate using PMMA solutions containing (*S*)-**BTPt** or TPE were investigated with the filter setup shown in Figure 4a. Changing the rotational angle from 45° to 135°, we found the color of the letter "P" written with PMMA solution containing (*S*)-**BTPT** turned from purple to orange. In contrast, the letter "t" written with PMMA solution containing TPE retained its cyan colour due to TPE emitting only nonpolarized luminescence. This result demonstrated the potential applications of **BTPt** in anti-counterfeiting and 4D visual recognition.

Conclusion

In summary, we found the assemblies of both (*R*)- and (*S*)-**BTPt** complexes in PMMA films were able to emit CPL with large g_{lum} values. Moreover, their CPL is able to display colour change by passing through a setup composed by a quarter-wave plate and a linear polarizer at different rotational angle between the plate and polarizer. Therefore, this CPL colour change was utilized as an additional dimension for colour coding, and "3D" code via doping PMMA films with (*R*)-**BTPt** replacing normal dyes demonstrated the different colour combinations at different rotational angles. The additional information for this "3D" code showed by these colour combinations

indicated the promising potential of CPL materials in 4D data encryption and anti-counterfeiting. This study indicates that replacing normal dyes with CPL dyes with large g_{lum} values to construct "3D" codes would be a new reliable approach to 4D coding and data encryption. Moreover, using CPL dyes with different colours and their enantiomers to construct "3D" codes would lead to more complicated CPL-based 4D codes, and make more space for their applications.

Experimental Sections

Materials and Methods

All commercially available solvents and chemicals were used as received without further purification unless otherwise indicated. The chiral pure (*R*)- and (*S*)-**BTPt** were supplied by Ms T. Gao and Mr. Z. Jiang with their kindness. Fluorescence spectra were determined using a Jobin–Yvon Horiba Fluoromax-4 spectrofluorimeter at room temperature. CPL spectra were recorded on a JASCO CPL-300 spectrofluoro polarimeter and using the simple moving average SMA method.

Luminescence spectra determination.

For luminescence spectra measurements, (*R*)-/(*S*)-**BTPt** in various solvents were measured with the following conditions: λ_{ex}, 380 nm; *c*, 1.0×10^{-5} mol L^{-1}, excitation and emission slit widths, 5 and 3 nm. (*R*)-/(*S*)-**BTPt** in DCM-hexane binary solvent systems were measured with similar conditions except for excitation and emission slit widths became 3 nm. Filters of 400 and 510 nm were used in sequence to avoid frequency doubling signals.

For the determination of (*R*)-/(*S*)-**BTPt** in PMMA films, PMMA powders (100 mg, d=1.188 gcm^{-1}) was dissolved in DCM (10 mL). Then different amounts of (*R*)-/(*S*)-**BTPt** were added into 1 mL of PMMA solution for mixing with ultrasonication (30 min). Then the PMMA films were prepared with a standard spin-coating procedure. Therefore, the cleaned quartz slides (20 mm × 10 mm × 1 mm) were placed on a spin coater. Then 100 μL of dye/PMMA mixture in DCM was added onto the plate with a pipette, and the film was formed via spin-coating at 1000 rpm for 90 s. The luminescence spectra of (*R*)-/(*S*)-**BTPt** in PMMA films on quartz plates

were measured upon excitation at 380 nm with both excitation and emission slit widths being of 2 nm. In the recording process, 400 nm and 510 nm filters were used in sequence to avoid frequency doubling signals.

CPL spectra determination.

For CPL spectra determination, (R)-/(S)-**BTPt** in DCM and hexane binary solvent systems were measured with following conditions: λ_{ex}, 380 nm; c, 1.0×10^{-4} mol L^{-1}, bandwidth, 1 nm; scanning speed, 100 nm min^{-1}; data pitch, 1 nm; CD scale, 10000 mdeg/1.0 doD, D.I.T., 2 s; excitation and emission slit widths, 3000 μm; accumulations, 5; cell length, 10 mm. For the determination of (*R*)-/(*S*)-**BTPt** in PMMA films, we used similar conditions except for the scanning speed was changed to 200 nm min^{-1} and accumulations became 3.

In the JASCO CPL-300 spectrofluoro polarimeter, the luminescence from the sample was measured at 180° with respect to the excitation-side monochromator, which is acceptable for measuring the g_{lum} values of **BTPt** in DCM-hexane binary solvent systems. Since the doped PMMA film samples are not transparent, for g_{lum} values of (*R*)-/(*S*)-**BTPt** in PMMA films, we determined based on the equation of $g_{lum}=2(I_L-I_R)/(I_L+I_R)$ using a fluorescence spectrofluorometer (Jobin–Yvon Horiba Fluoromax-4) modified with a rotatable quarter-wave plate (Thorlabs, WPQ05M-670) and a rotatable linear polarizer (Thorlabs, GT10-A). A CW Ozone-free xenon arc lamp (150 W) was utilized as a photoexcitation source. In this case, the luminescence from **BTPt**-doped films was measured at 90° with respect to the excitation-side monochromator. The left- and right-CPL from (*R*)-/(*S*)-**BTPt** assemblies pass through the rotatable quarter-wave retarder and a linear polarizer to enable the CPL signal detection. The detected luminescence intensity increases and decreases periodically via changing the rotational angle (θ) between the quarter-wave plate and the linear polarizer. The luminescence intensity obtained at θ of 45°, 225°, and 135°, 315° corresponds to the right- and left-CPL (I_R and I_L), respectively. The g_{lum} values were evaluated from 3 sets of measurements. The g_{lum} value of Cs[Eu((+)-hfbc)$_4$] (5×10^{-4} mol L^{-1}) in chloroform was determined as 1.39, which is consistent with that reported

in the literature.[11]

4D coding for data encryption and decryption

The PMMA films containing respectively (*R*)-/(*S*)-**BTPt**, TPE, and (*R*)-BM1 were prepared following the procedures described above. For 4D coding, the four films were joined together in the form described in Figure 6a caption for the decryption test. For the document security test, the two letters of the word "Pt", "P" and "t" were written respectively with in situ prepared PMMA solutions containing (*S*)-**BTPt** and TPE respectively.

The testing equipment setup was depicted in Figure 4a. In an optical platform, a rotatable quarter-wave plate (Thorlabs, WPQ05M-670) and a rotatable linear polarizer (Thorlabs, GT10-A), were placed in sequent before the sample. A laser pointer with an excitation wavelength of 395 nm was selected as the excitation source. The excitation light was designed to be perpendicular to luminescence direction passing through the quarter-wave retarder and linear polarizer. All the images were recorded using Nikon D7200.

Author contribution and acknowledgments

This work was supported by the National Talent Search Program for senior middle school students (C. He, supervisor: Prof. Z. Guo).

All experiments were designed and carried out under the guidance of Prof. Z. Guo with the help of Dr. Y. Chen and Mr. L. Xu. All the spectroscopic and 4D-coding studies were performed by C. He and T. Chen with equal contribution under the guidance of T. Gao and Z. Jiang. The draft was mainly composed by C. He based on the detailed discussion with T. Chen, Prof. Z. Guo, Dr. Y. Chen, Prof. Z. Liu and Mr. L. Xu, while T. Chen was responsible for all figures and diagrams. Prof. Z Guo and Mr. L. Xu helped to modify this manuscript in the final.

We also thank Ms. T. Gao, Mr. Z. Jiang for preparing the Pt complexes and offering the crystal structure information. Many thanks were given to Mr. Z. Jiang, who helped a lot in experiments and data presentation. We should express our special thanks to Prof. Z. Liu for his kind proposal on 4D code design and providing the experiment setup for 4D code readout.

本项工作受到国家中学生英才计划（何承堃，导师郭子建教授）以及国家自然

科学基金委的支持（郭子建）。

所有本文的实验工作均在南京大学郭子建院士指导下设计并完成，并受到陈韵聪博士的帮助。许亮亮老师在课题设计和要求方面给予了指导。何承堃和陈天弈共同参加并完成了荧光光谱、CPL 光谱和 4D 码等实验工作。其中陈天弈偏重溶液光谱研究，何承堃偏重薄膜光谱和 4D 码实验。在共同讨论基础上，何承堃负责论文初稿的主要撰写工作，陈天弈负责论文图片处理工作，并参与讨论和修改。论文由郭子建院士和许亮亮老师帮助完成修改。

特别感谢高婷婷和姜志勇制备了研究所用的铂配合物，并提供了晶体结构信息，为本文的研究提供了基础和出发点。感谢姜志勇在实验研究及数据展示方面的支持和帮助。特别感谢刘志鹏教授在四维码实验设计和设备方面的无私帮助。

References:

(1) Erevelles, S.; Fukawa, N.; Swayne, L. Big Data Consumer Analytics and the Transformation of Marketing. *J. Bus. Res.* **2016**, *69*, 897.

(2) Liu, X.; Wang, Y.; Li, X.; Yi, Z.; Deng, R.; Liang, L.; Xie, X.; Loong, D. T. B.; Song, S.; Fan, D.; All, A. H.; Zhang, H.; Huang, L.; Liu, X. Binary Temporal Upconversion Codes of Mn^{2+}-Activated Nanoparticles for Multilevel Anti-Counterfeiting. *Nat. Commun.* **2017**, *8*, 899.

(3) Wang,X.; Ma, H.; Gu, M.; Lin, C.; Gan, N.; Xie, Z.; Wang, H.; Bian, L.; Fu, L.; Cai, S.; Chi, Z.; Yao, W.; An, Z.; Shi, H.; Huang, W. Multicolor Ultralong Organic Phosphorescence through Alkyl Engineering for 4D Coding Applications, *Chem. Mater.* **2019**, *31*, 5584.

(4) Schadt, M. Liquid Crystal Materials and Liquid Crystal Displays. *Annu. Rev. Mater. Sci.* **1997**, *27*, 305.

(5) Wagenknecht, C.; Li, C.-M.; Reingruber, A.; Bao, X.-H.; Goebel, A.; Chen, Y.-A. Zhang, Q.; Chen, K.; Pan, J.-W. Experimental Demonstration of a Heralded Entanglement Source. *Nat. Photonics.* **2010**, *4*, 549.

(6) Farshchi, R.; Ramsteiner, M.; Herfort, J.; Tahraoui, A.; Grahn, H. T. Optical Communication of Spin Information between Light Emitting Diodes. *Appl. Phys. Lett.* **2011**, *98*, 162508.

(7) Sharma, V.; Crne,M.; Park, J. O.; Srinivasarao, M. Structural Origin of Circularly Polarized Iridescence in Jeweled Beetles, *Science*, **2009**, *325*, 449.

(8) Mori, T. *Circularly Polarized Luminescence of Isolated Small Organic Molecules*, Springer, Singapore, 2020.

(9) Sang, Y.; Han, J.; Zhao, T.; Duan, P.; Liu, M. Circularly Polarized Luminescence in Nanoassemblies:Generation, Amplification, and Application, *Adv. Mater.* **2019**, 1900110.

(10) Mei, J.; Leung, N. L. C.; Kwok, R. T. K.; Lam, J. W. Y.; Tang, B. Z. Aggregation-induced Emission: Together We Shine, United We Soar. *Chem. Rev.* **2015**, *115*, 11718.

(11) Lunkley, J. L.; Shirotani, D.; Yamanari, K.; Kaizaki, S.; Muller, G. Extraordinary Circularly Polarized Luminescence Activity Exhibited by Cesium tetrakis(3-heptafluoro-butylryl-(+)-camphorato)Eu(III) Complexes in EtOH and $CHCl_3$ Solutions. *J. Am. Chem. Soc.* **2008**, *130*, 13814.

(12) Lee, H.-E.; Ahn, H.-Y.; Mun, J.; Lee, Y. Y.; Kim, M.; Cho, N. H.; Chang, K.; Kim, W. S.; Rho, J. Nam, K. T. Amino-acid- and Peptide-Directed Synthesis of Chiral Plasmonic Gold Nanoparticles, *Nature*, **2018**, *556*, 360.

团队成员及指导教师简历

团队成员：

何承堃：男。南京外国语学校高三年级学生。热爱化学。2019 年底入选国家中学生英才计划（化学）。2020 年获加拿大化学竞赛和英国奥林匹克化学竞赛金奖。爱好篮球、流行音乐和化学实验。

陈天弈：女。南京外国语学校高三年级学生。热爱生命科学，在生物学奥林匹克竞赛中获国家二等奖，在 SAT2 数学、物理、化学考试中均获得满分。

指导教师：

郭子建：男。南京大学化学化工学院教授、博士生导师。中学生英才计划(化学)导师。1989-1994 年在意大利帕多瓦大学并获得博士学位。曾在英国伦敦大学、加拿大不列颠哥伦比亚大学、英国爱丁堡大学从事研究工作，研究方向为抗肿瘤金属配合物的作用机理研究。1999 年起担任南京大学教授、博士生导师。1999 年获得国家自然科学基金委杰出青年基金资助，2001 年被聘为教育部长江学者奖励计划特聘教授，2002 年被评为享受国务院特殊津贴专家，2017 年当选中国科学院化学部院士。曾任 Chem. Soc. Rev., Inorg. Chem., J. Biol. Inorg. Chem., 期刊的编委，目前担任 Coord. Chem. Rev., Dalton Trans., J. Inorg. Biochem., 等国际期刊的编委/顾问编委，以及《高等学校化学学报》、《无机化学学报》等刊物的副主编、主编。主要研究领域为金属化学生物学，研究方向包括：无机药物化学、金属-生物大分子相互作用机制以及生物无机物种的荧光识别与检测等。

许亮亮：男。2006 年硕士毕业于南京大学化学化工学院。南京外国语学校化学教师，江苏省“333 高层次人才培养工程”培养对象。2014 年“南京市优秀青年教师”。2012 年获得南京市高中化学优质课评比一等奖；2013 年获得江苏省化学优质课评比一等奖；2014 年获得全国高中化学优质课评比一等奖。2017 年 4 月获江苏省第六届化学创新实验大赛一等奖。在《化学教育 》、《化学教学》等全国中文核心期刊上发表论文 15 篇。2015 年主持江苏省教研室省级重点课题《基于技术素养视角培养学生实验创新能力的实践研究》。2017 年获得江苏省教学成果一等奖。2018 年获得全国教学成果一等奖。